Thin Solid Films 673 (2019) 57–61

Contents lists available at ScienceDirect

Thin Solid Films

journal homepage: www.elsevier.com/locate/tsf

Electronic excitations and optical properties of $YbFe_2O_4$ thin films

R.C. Rai[a,*], J. Hinz[a,1], M. Pascolini[a], F. Sun[b], H. Zeng[b]

[a] Department of Physics, SUNY Buffalo State, Buffalo, NY 14222, USA
[b] Department of Physics, University at Buffalo, SUNY, Buffalo, NY 14260, USA

ARTICLE INFO

Keywords:
Ytterbium ferrite
Thin film
Electronic excitation
Band gap

ABSTRACT

We present the structural, optical properties, and electronic excitation spectra of the $YbFe_2O_4$ thin film deposited on (0001) sapphire substrates. The optical spectra of a $YbFe_2O_4$ thin film show several electronic transitions, dominated by Fe *d* to *d* on-site electronic transitions as well as O 2*p* to Fe 3*d*, Yb 6*s*, and Yb 5*d* charge-transfer electronic transitions. The direct energy band gap of $YbFe_2O_4$ has been found to be 1.40 ± 0.01 eV at 300 K. Moreover, the electronic transitions centered at 1.75 eV and 2.41 eV exhibit strong temperature dependence with a discontinuity at ~190 ± 10 K, indicating evidence for a structural instability in the system. The optical spectra of $YbFe_2O_4$ have been analyzed and also compared with that of isostructural YFe_2O_4 and $LuFe_2O_4$.

1. Introduction

$YbFe_2O_4$ belongs to the RFe_2O_4 (R = Y, Dy to Lu) rare-earth ferrite family having the rhombohedral crystal structure ($R\bar{3}m$) [1] characterized by an alternating stacking of hexagonal double layer of FeO_5 bipyramids and RO_6 octahedra. This ferrite family has mixed valence iron with an equal number of Fe^{2+} and Fe^{3+} ions in a triangular lattice, resulting in both charge and spin frustrations in the system. As a result of the spin and charge frustrations, these ferrites exhibit unique magnetic properties, charge-ordered state, and spin-lattice coupling [2,4,3,5]. The ferrimagnetic transition due to the ordering of the Fe^{2+} and Fe^{3+} moments occurs around 250 K in this family. The charge-ordered state driven by the Fe^{2+} - Fe^{3+} charge interactions within the triangular lattice has been observed in $LuFe_2O_4$ [6,7,8,9] and in $YbFe_2O_4$ [10,12,13,14]. The ferroelectric polarization in $YbFe_2O_4$ has also been reported [11]. Moreover, $LuFe_2O_4$ and YFe_2O_4 undergo a structural distortion from a hexagonal structure to a monoclinic structure and then to a triclinic structure at T ~ 220 K and 190 K [15,16,17,18,19]..

The physical properties of the RFe_2O_4 oxides have been reported to be strongly sample dependent, revealing that the studies of these compounds are challenging [14,20,21,22,23]. For instance, both the three-dimensional and two-dimensional magnetic orderings have been observed in YFe_2O_4 and $LuFe_2O_4$, and such inconsistencies are believed to be caused by the amount of oxygen deficiencies in the samples [22,24,25,26]. Likewise, the ferroelectric property of $LuFe_2O_4$ is controversial for the same reason. Recently, Nagata et al. have reported the spontaneous electric polarization in $YbFe_2O_4$ [11]. This new result certainly brings attention to $YbFe_2O_4$. While the work on single crystal $YbFe_2O_4$ have been very limited, there are only a couple of studies on $YbFe_2O_4$ thin films [27,28]. Moreover, the systematic studies on the optical properties, the energy band gap, and the electronic excitations of the $YbFe_2O_4$ thin films are very important and clearly lacking. Optical spectroscopy offers a unique tool to investigate these properties of $YbFe_2O_4$ and help understand the multiferroic properties of this family of compounds.

In this letter, we report on the optical properties and electronic excitation spectra of $YbFe_2O_4$ thin films, deposited on (0001) sapphire substrates by a reactive electron beam deposition system. We measured the temperature-dependent optical spectra in the temperature range of 80–370 K using optical spectroscopy. We find that the optical spectra of $YbFe_2O_4$ contain several electronic excitations in the energy range 0.5–6.5 eV attributed to Fe^{2+} *d* to *d* on-site and O 2*p* to Fe 3*d* charge-transfer transitions. Based on the absorption spectra, $YbFe_2O_4$ has a direct energy band gap. In addition, we have analyzed the temperature dependence of the electronic excitations that shows subtle changes near the charge-ordering transition around ~300 K, and a discontinuity at ~190 K. We interpret that the observed optical feature at ~190 K is due to a structural instability in the system.

2. Experimental details

$YbFe_2O_4$ was prepared by a conventional solid state reaction. The powder samples of Yb_2O_3, Fe_2O_3, and FeO were mixed in a

* Corresponding author.
E-mail address: rairc@buffalostate.edu (R.C. Rai).
[1] Current address: Department of Physics and Astronomy, University of Rochester, Rochester, NY 14627, USA.

https://doi.org/10.1016/j.tsf.2019.01.035
Received 8 March 2018; Received in revised form 7 December 2018; Accepted 17 January 2019
Available online 24 January 2019

stoichiometric ratio and was thoroughly ground in mortal and pestal. The mixture was then pressed into pellets and sintered at 1100 °C for 15 h. After sintering, the process was repeated two more times: ground, pressed into pellets, and sintered. Finally, the prepared pellets were used as a target material for the electron beam deposition. Before thin film deposition, we preheated substrates at 600 °C for 30 min and slowly increased the substrate temperature to the final temperature. Similarly, the heating of the target pellet was carefully controlled by gradually increasing the electron beam power and raising the pellet temperature to allow the pellet surface to melt without any spattering of the material. We deposited 120 ± 10 nm [29] $YbFe_2O_4$ films on single crystal (0001) sapphire maintained at 800–850 °C with the film deposition rate of 90 Å/min. The film thickness was measured by a quartz crystal monitor during the deposition process. The chamber base pressure and the oxygen partial pressure were 2.5×10^{-4} Pa and 5×10^{-2} Pa, respectively, during the deposition. All as-grown thin films were annealed at 600 °C in the mixture of oxygen and air for about 3 h.

X-ray diffraction (XRD) and atomic force microscopy (AFM) have been employed to characterize the surface morphology and structural properties of the $YbFe_2O_4$ thin films. We measured variable-temperature (10–400 K) normal-incidence optical transmittance in the wavelength range of 190–3000 nm, with a spectral resolution of 1 nm, using a dual-beam spectrophotometer coupled with a continuous flow helium cryostat and a fiber optic spectrometer coupled with a closed-cycle helium refrigeration system. The magnetic data are measured using the Vibrating Sample Magnetometer option of a Physical Property Measurement System (Quantum Design).

3. Results and discussion

Fig. 1 (a) shows the XRD patterns of a 120 nm $YbFe_2O_4$ thin film grown at 800 °C on (0001) sapphire by a reactive electron beam deposition. The $YbFe_2O_4$ thin film on (0001) sapphire shows the (006), (107), (0012), and (0018) planes at 21.2°, 39.7°, 43.4°, and 67.4° respectively, as the preferred planes. Note that the two peaks observed at 20.5° and 41.7° correspond to the (0003) and (0006) planes of the substrate. Based on the XRD data, $YbFe_2O_4$ thin film is polycrystalline. No other phases were observed in the XRD pattern. Similarly, Fig. 1(b) shows 2μm x 2μm AFM image of the $YbFe_2O_4$ thin films on (0001) sapphire, annealed at 600 °C. The surface roughness of the thin film is relatively small with the root mean square value of ~7 nm.

The zero-field cooled (ZFC) and field cooled (FC) magnetization of the $YbFe_2O_4$-sapphire thin film as a function of temperature for H = 500 Oe (in the out-of-plane direction) is shown in Fig. 2 (a). The magnetic moment data do not show a clear magnetic transition, expected around 250 K (as shown in the inset for a close-up view), but the moment increases significantly below 100 K. Such increase in the

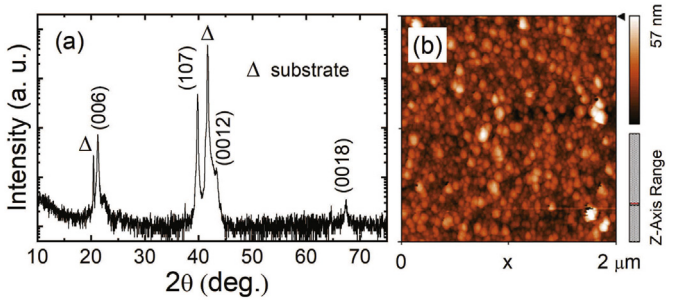

Fig. 1. (a) XRD pattern of a 120 nm $YbFe_2O_4$ thin film on (0001) sapphire substrate, showing the (006) and (107) planes, as the preferred crystalline orientation. The peaks at 20.5° and 41.8° are from the (0003) and (0006) planes of sapphire (b) AFM images (2μm × 2μm) of the $YbFe_2O_4$ thin film on sapphire substrate. The sample was annealed at 600 °C.

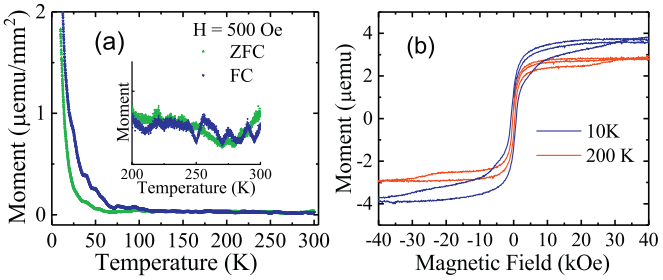

Fig. 2. Normalized magnetic moment of a 120 nm $YbFe_2O_4$ thin film as a function of (a) temperature for zero-field cooling and field cooling with H = 500 Oe. (b) magnetic field at 10 and 200. The M-H hysteresis loops at 10 and 200 K demonstrate a ferrimagnetic behavior.

moment at low temperatures has been observed in single crystal $YbFe_2O_4$ which is attributed to the moments of Yb^{3+} ions [30,31]. As shown in Fig. 2 (b), the sample demonstrates a hysteresis effect at 200 K and 10 K, consistent with the expected ferrimagnetic state of $YbFe_2O_4$ below the magnetic transition temperature. The hysteresis loop disappears at room temperature (not shown), as expected in the paramagnetic state. The coercivity and the saturation magnetization values at 10 K are about 25% higher than their values at 200 K.

Fig. 3 (a) shows room temperature near-normal reflectance and transmittance of a 120 nm $YbFe_2O_4$ film on sapphire. The spectra show an interference effect below 2.0 eV while the absorption increases rapidly above 2.0 eV. In order to investigate the optical properties and the electronic excitations of $YbFe_2O_4$, we extracted the absorption coefficient (α) from the measured transmittance and reflectance of the $YbFe_2O_4$ thin film at 300 K (as shown in Fig. 3(b)) using $\alpha = -(1/d)\ln[T/(1-R)]$, where d is the film thickness, R is the reflectance, and T is the transmittance. Then, the absorption spectrum has been fitted with the peak fitting software to identify the electronic transitions. For the fitting, the Gaussian-amplitude function was used, and the best fit (green line) was obtained with 5 peaks as indicated by the solid lines.

The absorption spectrum of $YbFe_2O_4$ contains the electronic

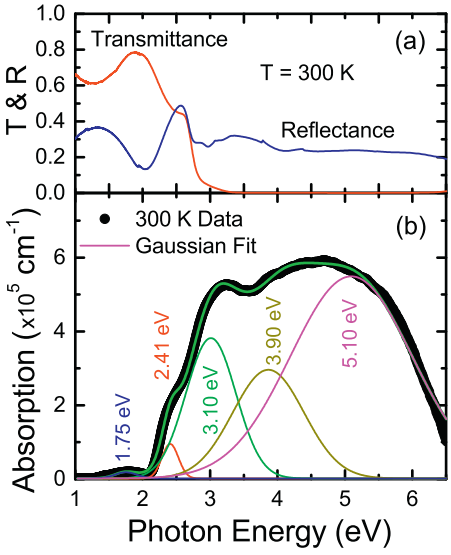

Fig. 3. (a) Room temperature transmittance and reflectance as a function of photon energy of a 120 nm $YbFe_2O_4$ film on sapphire. (b) The absorption coefficient (α) of the $YbFe_2O_4$ thin film at 300 K, extracted from the measured transmittance and reflectance. A solid line (green) represents the peak fitting for the absorption (solid circle) with 5 peaks as indicated by the solid lines. The Gaussian function was used for the peak fitting process. (For interpretation of the references to colour in this figure legend, the reader is referred to the web version of this article.)

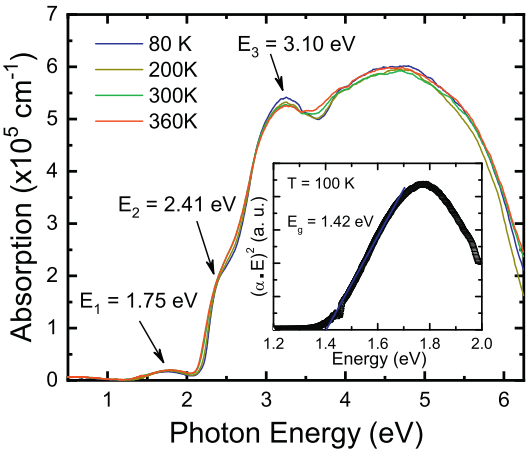

Fig. 4. Representative absorption spectra of a 120 nm $YbFe_2O_4$ film on sapphire at 80, 200, 300, 360 K, respectively. The three electronic transitions associated with Fe^{2+} *d* to *d* and O 2*p* to Fe 3*d*, as indicated by the arrows, were studied for their temperature dependence. The inset shows the $(\alpha. E)^2$ versus Photon Energy for a $YbFe_2O_4$ thin film at 100 K. The solid line represents the direct band gap model fitting of the data to extract the energy band gap (E_g ~1.42 ± 0.01 eV).

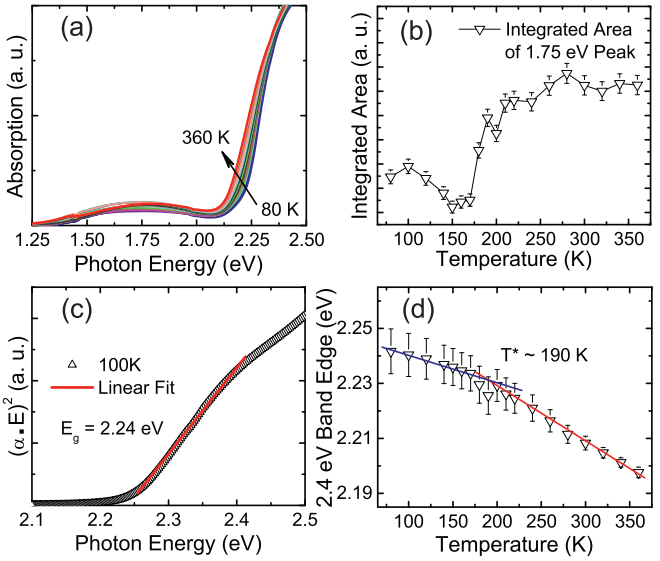

Fig. 5. (a) A close-up view of the absorption spectra in the low-energy region for the $YbFe_2O_4$ thin film between 80 and 360 K. (b) Temperature dependence of the integrated area of the 1.75 eV peak. (c) $(\alpha. E)^2$ versus Energy for the upper energy band gap of $YbFe_2O_4$ at 100 K. A solid line represents the fitting of the graph using the direct energy band gap model. (d) Temperature dependence of the absorption edge of the 2.41 eV electronic transition, indicating a discontinuity at ~190 K. The solid lines are guides to the eye.

excitations at ~1.75 eV, 2.41 eV, 3.10 eV, 3.90 eV, and 5.10 eV, and these electronic excitations are very similar to that of isostructural $LuFe_2O_4$ and YFe_2O_4 thin films [32,33]. Based on the electronic transitions of $LuFe_2O_4$, the two weaker peaks near ~1.75 eV and 2.41 eV are attributed to the Fe^{2+} ($3d^6$) *d* to *d* electronic excitations. In general, the *d* to *d* on-site excitations are parity forbidden and as a result, these excitations have weak oscillator strengths. In this family of rare-earth iron oxides, we have found that the local distortion, the spin-lattice coupling, and a strong hybridization between O 2*p* and Fe 3*d* states in the building block FeO_5 [34,35], are very common phenomena. Consequently, the *d* orbitals are not purely of *d* characteristics rather they are the *p-d* hybridized orbitals, and the two weaker peaks at 1.75 eV and 2.41 eV originate from the electronic excitations from the *p-d* hybridized states to the empty Fe 3*d* states. Similarly, the three stronger peaks centered at ~3.10 eV. 4.8 eV, and 5.10 eV are assigned to O 2*p* to Fe 3*d*, Yb 5*d*, and Yb 6*s* charge-transfer excitations.

Fig. 4 shows representative absorption spectra of a 120 nm $YbFe_2O_4$ film as a function of photon energy between 80 K and 370 K. While the transmittance was measured at different temperatures, the reflectance was measured only at 300 K, and the same 300 K reflectance was used to extract all absorption coefficients. The use of the reflectance data help eliminate the interference peak below 1.75 eV, but it does not affect the high energy features. The inset (Fig. 4) shows an example of the energy band gap extraction from the $(\alpha. E)^2$ versus Photon Energy for the $YbFe_2O_4$ thin film at 100 K. The fitting of the data gives the direct energy band gap of $YbFe_2O_4$ to be E_g ~1.42 ± 0.01 eV at 100 K [36]. The fitting (not shown) with the indirect energy gap model did not show two slopes expected from the model, and thus we conclude that $YbFe_2O_4$ has a direct energy band gap. Although the 120 nm $YbFe_2O_4$ thin film data show a direct energy band gap, we cannot discount the fact that our data may not have sensitivity to an indirect gap due to the film thickness. We note that the thicker film and a single crystal samples will offer a better insight into the true nature of the energy gap in this material. Further, the energy band gap does not change much at low temperatures. For example, the value of E_g slightly increased from ~1.40 eV at 300 K to ~1.42 eV at 80 K. It is interesting to note that the intensity of the 1.75 eV peak decreases on cooling (discussed below).

The temperature dependence of the electronic excitations can offer insight into the structural distortion and the coupling between the spin and charge degrees of freedom in this frustrated magnetic system. Fig. 5 (a) shows the close-up view of the low-energy excitations centered at ~1.75 eV and 2.41 eV for the $YbFe_2O_4$ thin film in the temperature range 80–360 K. It is clear that these excitations exhibit a strong temperature dependence. Particularly, the oscillator strength of the 1.75 eV peak becomes weaker and the rising slope of the 2.41 eV peak shifts to higher energies on cooling. To elaborate the temperature dependence of the intensity of the electronic transition, we integrated the 1.75 eV peak and plotted as a function of temperature, as shown in Fig. 5(b). As shown, the integrated area significantly decreases below 190 K, which is an indication of the changes in the crystal-field environment of Fe ions. We interpret that the modifications of the crystal-field environment is associated with a structural instability. Such instability in the magnetic state could arise from the coupling among the spin, lattice, and charge degrees of freedom. In addition, the integrated area shows a subtle change at ~250 K which could be attributed to the onset of the magnetic ordering in the system.

As shown in Fig. 5 (a), the oscillator strength of the 2.41 eV peak is much stronger than that of the 1.75 eV peak. Although the fundamental energy band gap of $YbFe_2O_4$ is related to the electronic transition at 1.75 eV, the energy band edge of the 2.41 eV peak is referred to as the upper energy band gap. We have extracted the upper energy band gap by fitting the $(\alpha. E)^2$ versus Energy data at each temperature with the direct-type energy gap model. An example of the 100 K data fitting is shown in Fig. 5(c). In Fig. 5(d), we show the 2.41 eV band edge extracted from the fitting as a function of temperature. As shown, the band edge exhibits two linear regions with a discontinuity at 190 ± 10 K. Between 360 K and 190 K, the data suggest that the band edge increases (i.e. blueshift) at a faster rate while the rate of increase slows down below 190 K. The observed temperature dependence of the energy band strongly suggests that the building block FeO_5 trigonal bipyramids may have undergone through a structural instability below 190 K. It is noted that $LuFe_2O_4$ and YFe_2O_4 undergo a structural change from a hexagonal structure to a monoclinic/triclinic structure below 180 K, which is attributed to the spin and charge frustrations in the lattice [3,24,37,38,39]. We have also reported such structural distortion in $LuFe_2O_4$ and YFe_2O_4 thin films [32,33]. A recent study on single crystal $YbFe_2O_4$ suggests that, besides its paramagnetic to ferrimagnetic

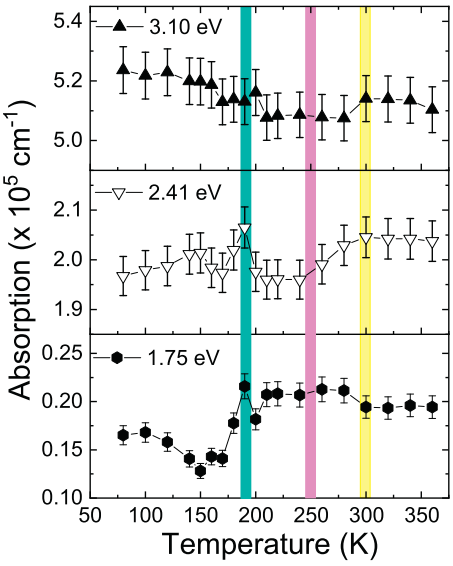

Fig. 6. Temperature dependence of three electronic excitations centered at 1.75, 2.41 and 3.10 eV of a $YbFe_2O_4$ thin film. The shaded vertical lines designate a structural instability at $T^* \sim 190$ K, the magnetic transition at $T_N \sim 240$ K, and the charge-ordering transition at $T_{CO} \sim 300$ K.

transition at 255 K, this compound undergoes a ferrimagnetic (fM) to an antiferromagnetic (AFM) transition at ~210 K and it further goes into a low temperature phase at 139 K [10]. In this context, the observed discontinuity around 190 K in the $YbFe_2O_4$ thin film could be associated with the changes in the spin structures in the system. It is noted that $YbFe_2O_4$ thin film is strained in addition to the frustrations in the system, likely causing the structural instability. A structural instability could directly affect the building block FeO_5 trigonal bi-pyramids i.e., the crystal-field environment of Fe ions, consequently manifesting as a discontinuity in the temperature dependence of the electronic excitations.

We further analyzed the temperature dependence of the electronic excitations in order to explore the structural instability. In Fig. 6, we show the temperature dependence of the peak position of the three electronic excitations located at 1.75 eV, 2.41 eV, and 3.10 eV. Overall, the peak intensity of the 1.75 eV and 2.41 eV excitations decreases upon cooling. In contrast, the 3.10 eV peak intensity increases at low temperatures. Moreover, the 1.75 eV and 2.41 eV peaks show a significant drop in their intensities below 190 K. The discontinuity in the peak positions around 190 K, which is consistent with the temperature dependence of the integrated area in Fig. 5(b), supports the argument that the crystal structure of $YbFe_2O_4$ is unstable through the magnetic transition. The peak intensities, however, do not show any clear changes around ~250K with the onset of the ferrimagnetic ordering in $YbFe_2O_4$. On the other hand, the peak intensity of the three peaks display the changes around ~300 K which possibly indicate the charge-ordering transition in the system [37]. We speculate that the spin frustrations cause the structural instability at low temperatures, and consequently leading to a strong temperature dependence of the optical properties and the electronic excitations in the family of RFe_2O_4 (R = Y, Yb, and Lu) thin films.

4. Conclusion

In summary, we investigated the structure, optical properties, and electronic excitations of the polycrystalline $YbFe_2O_4$ thin films. The optical spectra of $YbFe_2O_4$ show Fe *d* to *d* on-site transitions at 1.75 eV and 2.41 eV, while the charge-transfer transitions from O 2*p* to Fe 3*d*, Yb 5*d*, and Yb 6*s* are located at 3.10 eV, 3.90 eV, and 5.10 eV, respectively. These electronic transitions are consistent with that of the $LuFe_2O_4$ and YFe_2O_4 thin films. The direct energy band gap of $YbFe_2O_4$ has been found to be 1.40 ± 0.01 eV at 300 K. Likewise, the temperature dependence of the three electronic transitions centered at 1.75 eV, 2.41 eV, and 3.10 eV indicates a structural instability at ~190 ± 10 K.

Acknowledgments

Work at SUNY Buffalo State was supported by the National Science Foundation (DMR-1406766). Work at University at Buffalo was supported by the National Science Foundation (DMR-1104994 and CBET-1510121).

References

[1] K. Kato, I. Kawada, N. Kimizuka, T. Katsura, Crystal-structure of $YbFe_2O_4$, Zeitschrift Fur Kristallographie 141 (1975) 314, https://doi.org/10.1524/zkri.1975.141.3-4.314.
[2] N. Ikeda, H. Ohsumi, K. Ohwada, K. Ishii, T. Inami, K. Kakurai, Y. Murakami, K. Yoshii, S. Mori, Y. Horibe, H. Kito, Ferroelectricity from iron valence ordering in the charge-frustrated system $LuFe_2O_4$, Nature 436 (2005) 1136, https://doi.org/10.1038/nature04039.
[3] A. Nagano, M. Naka, J. Nasu, S. Ishihara, Electric polarization, magnetoelectric effect and orbital state of a layered iron oxide with frustrated geometry, Phys. Rev. Lett. 99 (2007) 217202, https://doi.org/10.1103/PhysRevLett.99.217202.
[4] J. van den Brink, D.I. Khomskii, Multiferroicity due to charge ordering, J. Phys.: Condens. Matter 20 (2008) 434217, https://doi.org/10.1088/0953-8984/20/43/434217.
[5] Makoto Naka, Aya Nagano, Sumio Ishihara, Magnetodielectric phenomena in a charge- and spin-frustrated system of layered iron oxide, Phys. Rev. B 77 (2008) 224441, https://doi.org/10.1103/PhysRevB.77.224441.
[6] J. Lee, S.A. Trugman1, C.D. Batista, C.L. Zhang, D. Talbayev, X.S. Xu, S.-W. Cheong, D.A. Yarotski, A.J. Taylor, R.P. Prasankumar, Probing the interplay between quantum charge fluctuations and magnetic ordering in $LuFe_2O_4$, Sci. Rep. 3 (2013) 2654, https://doi.org/10.1038/srep02654.
[7] F. Sun, R. Wang, C. Aku-Leh, H.X. Yang, R. He, J.M. Zhao, Double charge ordering states and spin ordering state observed in a RFe_2O_4 system, Sci. Rep. 4 (2014) 6429, https://doi.org/10.1038/srep06429.
[8] D.H. Kim, J. Hwang, E. Lee, J. Kim, B.W. Lee, H.-K. Lee, J.-Y. Kim, S.W. Han, S.C. Hong, C.-J. Kang, B.I. Min, J.-S. Kang, Interplay between R 4f and Fe 3d states in charge-ordered RFe_2O_4 (R = Er, Tm, Lu), Phys. Rev. B 87 (2013) 184409, https://doi.org/10.1103/PhysRevB.87.184409.
[9] I.K. Yang, J. Kim, S.H. Lee, S.-W. Cheong, Y.H. Jeong, Charge ordering, ferroelectric, and magnetic domains in $LuFe_2O_4$ observed by scanning probe microscopy, Appl. Phys. Lett. 106 (2015) 152902, https://doi.org/10.1063/1.4918358.
[10] H.L. Williamson, T. Mueller, M. Angst, G. Balakrishnan, Growth of $YbFe_2O_4$ single crystals exhibiting long-range charge order via the optical floating zone method, J. Cryst. Growth 475 (2017) 44, https://doi.org/10.1016/j.jcrysgro.2017.05.034.
[11] T. Nagata, P.-E. Janolin, M. Fukunaga, B. Roman, K. Fujiwara, H. Kimura, J.-M. Kiat, N. Ikeda, Electric spontaneous polarization in $YbFe_2O_4$, Appl. Phys. Lett. 110 (2017) 052901, , https://doi.org/10.1063/1.4974994.
[12] Y. Murakami, N. Abe, T. Arima, D. Shindo, Charge-ordered domain structure in $YbFe_2O_4$ observed by energy-filtered transmission electron microscopy, Phys. Rev. B 76 (2007) 024109, https://doi.org/10.1103/PhysRevB.76.024109.
[13] A.J. Hearmon, D. Prabhakaran, H. Nowell, F. Fabrizi, M.J. Gutmann, P.G. Radaelli, Helical scattering signatures of strain and electronic textures in $YbFe_2O_4$ from three-dimensional reciprocal-space imaging, Phys. Rev. B 85 (2012) 014115, https://doi.org/10.1103/PhysRevB.85.014115.
[14] H. Kobayashi, K. Fujiwara, N. Kobayashi, T. Ogawa, M. Sakai, M. Tsujimoto, O. Seri, S. Mori, N. Ikeda, Stability of cluster glass state in nano order sized $YbFe_2O_4$ powders, J. Phys. Chem. Solids 103 (2017) 103, https://doi.org/10.1016/j.jpcs.2016.12.014.
[15] S. Lafuerza, J. Garcia, G. Subias, J. Blasco, V. Cuartero, Strong local lattice instability in hexagonal ferrites RFe_2O_4 (R = Lu, Y, Yb) revealed by x-ray absorption spectroscopy, Phys. Rev. B 89 (2014) 045129, https://doi.org/10.1103/PhysRevB.89.045129.
[16] Y. Nakagawa, M. Inazumi, N. Kimizuka, K. Siratori, Low-temperature phase transitions and magnetic properties of YFe_2O_4, J. Phys. Soc. Jpn. 47 (1979) 1369, https://doi.org/10.1143/jpsj.47.1369.
[17] M. Inazumi, Y. Nakagawa, M. Tanaka, N. Kimizuka, K. Shiratori, Magnetizations and mssbauer spectra of YFe_2O_{4-x}, J. Phys. Soc. Jpn 50 (1981) 438, https://doi.org/10.1143/jpsj.50.438.
[18] M. Tanaka, J. Akimitsu, Y. Inada, N. Kimizuka, I. Shindo, K. Siratori, Conductivity and specific heat anomalies at the low temperature transition in the stoichiometric YFe_2O_4, Solid State Commun. 44 (1982) 687, https://doi.org/10.1016/0038-1098(82)90583-X.
[19] I. Naoshi, N. Tomoko, K. Jun, M. Shigeo, Present status of the experimental aspect of RFe_2O_4 study, J. Phys.: Condens. Matter 27 (2015) 053201, https://doi.org/10.1088/0953-8984/27/5/053201.
[20] S. Mori, S. Shinohara, Y. Matsuo, Y. Horibe, K. Yoshii, N. Ikeda, Effect of oxygen vacancies on charge ordered structure in $YFe_2O_{4-\delta}$, Jpn. J. of Appl. Phys. 47 (2008) 7595, https://doi.org/10.1143/jjap.47.7595.

[21] Y. Horibe, K. Kishimoto, S. Mori, N. Ikeda, Dielectric anomaly and structural phase transitions in $YFe_2O_{4-\delta}$, Integr. Ferroelectrics 67 (2004) 151, https://doi.org/10.1080/10584580490898876.
[22] F. Wang, J. Kim, G.D. Gu, Y. Lee, S. Bae, Y.-J. Kim, Oxygen stoichiometry and magnetic properties of $LuFe_2O_{4-\delta}$, J. Appl. Phys. 113 (2013) 063909, https://doi.org/10.1063/1.4792036.
[23] M. Hervieu, A. Guesdon, J. Bourgeois, E. Elkaim, M. Poienar, F. Damay, J. Rouquette, A. Maignan, C. Martin, Oxygen storage capacity and structural flexibility of $LuFe_2O_{4-\delta}$, Nat. Mater. 13 (2014) 74, https://doi.org/10.1038/nmat3809.
[24] J. Akimitsu, Y. Inada, K. Siratori, I. Shindo, N. Kimizuka, Two-dimensional spin ordering in YFe_2O_4, Solid State Commun. 32 (1979) 1065, https://doi.org/10.1016/0038-1098(79)90831-7.
[25] H.X. Yang, H.F. Tian, Z. Wang, Y.B. Qin, C. Ma, J.Q. Li, Z.Y. Cheng, R. Yu, J. Zhu, Effect of oxygen stoichiometry in $LuFe_2O_{4-\delta}$ and its microstructure observed by aberration-corrected transmission electron microscopy, J. Phys.: Condens. Matter 24 (2012) 435901, https://doi.org/10.1088/0953-8984/24/43/435901.
[26] T. Michiuchi, Y. Yokota, T. Komatsu, H. Hayakawa, T. Kuroda, D. Maeda, Y. Matsuo, S. Mori, K. Yoshii, N. Hanasaki, T. Kambe, N. Ikeda, Stoichiometric study of the dielectric and magnetic properties in charge frustrated system $LuFe_2O_4$, Ferroelectrics 378 (2009) 175, https://doi.org/10.1080/00150190902859187.
[27] T. Fujii, N. Okamura, H. Hashimoto, M. Nakanishi, J. Kano, N. Ikeda, Structural, magnetic and optical properties of $YbFe_2O_4$ films deposited by spin coating, AIP Advances 6 (2016) 8, https://doi.org/10.1063/1.4961639.
[28] R. Kashimoto, T. Yoshimura, A. Ashida, N. Fujimura, Lowering the growth temperature of strongly-correlated $YbFe_2O_4$ thin films prepared by pulsed laser deposition, Thin Solid Films 614 (2016) 44, https://doi.org/10.1016/j.tsf.2016.04.044.
[29] For the purpose of thickness measurement, we also fitted the reflectance and transmittance spectra of the $YbFe_2O_4$thin film simultaneously using the Tauc-Lorenzt model. From the fitting, the thickness was estimated to be 123 nm, which is consistent with the quartz crystal monitor value of ~120 nm.
[30] Y. Sun, Y. Liu, F. Ye, S. Chi, Y. Ren, T. Zou, F. Wang, L. Yan, A magnetoelectric multiglass state in multiferroic $YbFe_2O_4$, J. Appl. Phys. 111 (2012) 07D902, https://doi.org/10.1063/1.3670969.
[31] K. Yoshii, D. Matsumura, H. Saitoh, T. Kambe, M. Fukunaga, Y. Muraoka, N. Ikeda, S. Mori, Current-induced enhancement of magnetic anisotropy in spin-charge-coupled multiferroic $YbFe_2O_4$, J. Phys. Soc. Jpn. 83 (2014) 063708, https://doi.org/10.7566/JPSJ.83.063708.
[32] R.C. Rai, A. Delmont, A. Sprow, B. Cai, M.L. Nakarmi, Spin-charge-orbital coupling in multiferroic $LuFe_2O_4$ thin films, Appl. Phys. Lett. 100 (2012) 212,904, https://doi.org/10.1063/1.4720401.
[33] R.C. Rai, J. Hinz, G.X.A. Petronilo, F. Sun, H. Zeng, M.L. Nakarmi, P.R. Niraula, Signature of structural distortion in optical spectra of YFe_2O_4 thin film, AIP Advances 6 (2016) 025021, https://doi.org/10.1063/1.4942753.
[34] H.J. Xiang, M.H. Whangbo, Charge order and the origin of giant magnetocapacitance in $LuFe_2O_4$, Phys. Rev. Lett. 98 (2007) 246403, https://doi.org/10.1103/PhysRevLett.98.246403.
[35] K. Kuepper, M. Raekers, C. Taubitz, M. Prinz, C. Derks, M. Neumann, A.V. Postnikov, F.M.F. de Groot, C. Piamonteze, D. Prabhakaran, S.J. Blundell, Charge order, enhanced orbital moment, and absence of magnetic frustration in layered multiferroic $LuFe_2O_4$, Phys. Rev. B 80 (2009) 220,409, https://doi.org/10.1103/PhysRevB.80.220409.
[36] The energy band gap (~1.40 eV at 300 K) of the $YbFe_2O_4$ thin film is smaller than that of a 300 nm $LuFe_2O_4$ thin film [Ref. 32] with ~2.18 eV. Similarly, Brooks et al. [Appl. Phy. Lett. **101**, 132,907 (2012)] have reported an indirect band gap ($Fe^{2+} \rightarrow Fe^{3+}$ charge transfer) of 0.35 ev and a direct band gap (O $p \rightarrow$ Fe d charge transfer) of 3.4 eV, respectively, for a 75 nm $LuFe_2O_4$ thin film.
[37] J. Blasco, S. Lafuerza, J. Garcia, G. Subias, Structural properties in RFe_2O_4 compounds (R = Tm, Yb, and Lu), Phys. Rev. B 90 (2014) 11, https://doi.org/10.1103/PhysRevB.90.094119.
[38] A.D. Christianson, M.D. Lumsden, M. Angst, Z. Yamani, W. Tian, R. Jin, E.A. Payzant, S.E. Nagler, B.C. Sales, D. Mandrus, Three-dimensional magnetic correlations in multiferroic $LuFe_2O_4$, Phys. Rev. Lett. 100 (2008) 107601, https://doi.org/10.1103/PhysRevLett.100.107601.
[39] M. Angst, R.P. Hermann, A.D. Christianson, M.D. Lumsden, C. Lee, M.H. Whangbo, J.W. Kim, P.J. Ryan, S.E. Nagler, W. Tian, R. Jin, B.C. Sales, D. Mandrus, Charge order in $LuFe_2O_4$: antiferroelectric ground state and coupling to magnetism, Phys. Rev. Lett. 101 (2008) 227601, https://doi.org/10.1103/PhysRevLett.101.227601.